Deletion of the inflammatory S100-A9/MRP14 protein does not influence survival in hSOD1 G93A ALS mice

Matthieu Ribon, Céline M Leone, Aude Chiot, Félix Berriat, Martine Rampanana, Julie Cottin, Delphine Bohl, Stéphanie Millecamps, Christian S. Lobsiger, Michael T. Heneka, et al.

Deletion of the inflammatory S100-A9/MRP14 protein does not influence survival in hSOD1^{G93A} ALS mice

Matthieu Ribon[1], Céline Leone[1]*, Aude Chiot[1]*, Félix Berriat[1], Martine Rampanana[1], Julie Cottin[1], Delphine Bohl[1], Stéphanie Millecamps[1], Christian S. Lobsiger[1], Michael T. Heneka[2], Séverine Boillée[1]*

[1]Sorbonne Université, Institut du Cerveau - Paris Brain Institute - ICM, Inserm, CNRS, Paris, France.

[2]Department of Neurodegenerative Disease and Gerontopsychiatry/Neurology, University of Bonn Medical Center, 53127 Bonn, Germany; German Center for Neurodegenerative Diseases (DZNE), 53127 Bonn, Germany

* these authors contributed equally

Corresponding author: Séverine Boillée, severine.boillee@sorbonne-universite.fr

Abstract.

Neuroinflammation is a hallmark of Amyotrophic Lateral Sclerosis (ALS) in hSOD1^{G93A} mouse models where microglial cells contribute to the progressive motor neuron degenerative process. S100-A8 and S100-A9 (also known as MRP8 and MRP14, respectively) are cytoplasmic proteins expressed by inflammatory myeloid cells, including microglia and macrophages. Mainly acting as a heterodimer, S100-A8/A9, when secreted, can activate Toll-like Receptor 4 on immune cells, leading to deleterious proinflammatory cytokine production. Deletion of S100a9 in Alzheimer's disease mouse models showed a positive outcome, reducing pathology. We now assessed its role in ALS. Unexpectedly, our results show that deleting S100a9 in hSOD1^{G93A} ALS mice had no impact on mouse survival, but rather accelerated symptoms with no impact on microglial activation and motor neuron survival, suggesting that blocking S100-A9 would not be a valuable strategy for ALS.

Key words: S100a9/MRP14, Calgranulin B, DAMP, neuro-inflammation, ALS

1. Introduction

Amyotrophic Lateral Sclerosis (ALS) is the most common, adult onset, motor neuron disease leading to fatal paralysis. While microglial cells, the macrophages of the central nervous system are involved in disease progression, microglial cell pathways involved in motor neuron death remain largely unidentified (Beers et al., 2006; Boillée et al., 2006). S100-A8 (also known as MRP8) and S100-A9 (also known as MRP14 or Calgranulin B) are cytoplasmic proteins of the S100 calcium binding protein family, implicated in cytoskeleton remodeling, crucial for cell migration and phagocytosis. S100-A8 and S100-A9 are mainly expressed by myeloid cells and overexpressed during inflammation (Akiyama et al., 1994; Wang et al., 2018). Although some anti-inflammatory properties have been reported, they are secreted as danger-associated molecular pattern signals. They form a heterocomplex (S100-A8/A9 called calprotectin) inducing Toll-like Receptor-4 (TLR4) responses that leads to deleterious proinflammatory cytokine release (Donato et al., 2013; Ehrchen et al., 2009; Vogl et al., 2007; Wang et al., 2018). Deleting S100a9 in Alzheimer's disease (AD) mouse models leads to increased capacity of microglia to phagocytose amyloid plaques and decreased memory impairment (Akiyama et al., 1994; Kim et al., 2014; Kummer et al., 2012). Although extracellular deposits are not present in ALS, secretion of misfolded mutant SOD1 or its release through extracellular vesicles are suspected to contribute to disease spreading (Silverman et al., 2016; Urushitani et al., 2006). In addition, S100-A8/A9 contributes to damage in focal ischemia through microglial recruitment and activation at a (sterile) inflammation site (Ziegler et al., 2009). Based on this data indicating a role of S100-A8/A9 in several models of neuroinflammation, and existing evidence suggesting disease contribution of neuroinflammatory reactions in ALS, we deleted S100a9 in hSOD1^{G93A} ALS mice to uncover whether S100-A8/A9 would be involved in the mutant SOD1-mediated ALS toxicity and could represent a potential microglial target to increase motor neuron survival.

2. Methods

See supplementary material for extended methods. Mice from the three different genotypes (hSOD1^{G93A}:S100a9+/+, hSOD1^{G93A}:S100a9+/-, hSOD1^{G93A}:S100a9-/-) were true littermates, obtained through a two-step mating strategy between hSOD1^{G93A} (Gurney et al., 1994) and S100a9-/- mice (Manitz et al., 2003), both on a C57BL/6 background. Mice were weighed and their grip-strength measured weekly from the presymptomatic stage (50 days of age) to disease end stage (complete hindlimb paralysis, around 165 days), with onset (weight or grip strength peak) and symptomatic (10% of weight loss or 35% of grip-strength loss (Chiot et al., 2020; Mesci et al., 2015)) stages determined retrospectively. At least 20 mice per genotype (gender balance) were used for the survival analysis. Lumbar spinal cords and sciatic nerves were collected at each time point from 3–4 mice per genotype (gender balance) to perform immunostainings for microglial cells (Iba1), to stain motor neurons for quantification (Nissl staining, cresyl-violet-acetate) and for RT-qPCR analysis of S100a8 and S100a9 (with Actg1, gamma-actin, as a normalizer).

3. Results

3.1. S100a8 and S100a9 mRNA expression levels are not modified in lumbar spinal cords but are increased at disease end stage in sciatic nerves of ALS mice.

S100a8 and S100a9 mRNAs being enriched in macrophages/microglia (Zhang et al., 2014), we measured S100a8 and S100a9 mRNA expression in lumbar spinal cord and sciatic nerve tissues of ALS mice, which shows increased microglial and peripheral nerve macrophage activation, throughout the disease. S100a8 and S100a9 mRNA levels were stable in the spinal cord (with the trend toward downregulation at the symptomatic stage, (Fig. 1 A and B)). In sciatic nerves, S100a8 and S100a9 mRNA levels increased at disease end stage compared to the presymptomatic stage (Fig. 1 C and D).

3.2. Deleting S100a9 in ALS mice does not modify hSOD1^{G93A} ALS mouse survival but slightly accelerates the appearance of disease symptoms.

To determine the role of the S100-A8/A9 complex on the ALS disease course (and since S100a8 KO mice are embryonic lethal (Passey et al., 1999)), we deleted S100a9 in hSOD1^{G93A} mice. While (littermate) hSOD1^{G93A}:S100a9-/- and hSOD1^{G93A}:S100a9+/+ mice had similar maximum weight and grip-strength (Supplementary Fig. 1), and hSOD1^{G93A}:S100a9-/- mice reached disease onset, defined by weight peak, at the same age than hSOD1^{G93A}:S100a9 +/+ mice (Fig. 2 A), there was a trend that hSOD1^{G93A}:S100a9-/- mice reached onset, defined by grip-strength peak, slightly earlier than hSOD1^{G93A}:S100a9+/+ mice (Fig. 2 A'). The same trend was also observed for the symptomatic stage (Fig. 2 B and B'). However, hSOD1^{G93A}:S100a9-/- and hSOD1^{G93A}:S100a9+/+ mice reached disease end stage both at the same age (Fig. 2 C). However, the duration of the late phase (defined by weight) was shorter in hSOD1^{G93A}:S100a9-/- compared to hSOD1^{G93A}:S100a9 +/+ mice (Fig. 2 D). Indeed, disease was accelerated from the symptomatic stage (defined by 10% of weight loss) onward (Fig. 2 E). Of note, mice with deletion of only one copy of S100a9 (hSOD1^{G93A}:S100a9+/-), showed similar results as hSOD1^{G93A}:S100a9+/+ mice.

3.3. Microglial activation and motor neuron survival are not affected by S100a9 deletion in hSOD1^{G93A} mice.

Microglial activation measured by Iba1+ immunoreactive area in the lumbar spinal cord (Fig. 3 A) was increased in symptomatic hSOD1^{G93A} mice, but regardless of S100a9 expression, without difference between hSOD1^{G93A}:S100a9-/- and hSOD1^{G93A}:S100a9 +/+ mice (Fig. 3 A and B). In addition, while motor neurons progressively degenerated throughout the disease, motor neuron numbers were similar in hSOD1^{G93A}:S100a9-/- and hSOD1^{G93A}:S100a9 +/+ mice at equivalent disease stages, (except for a minor difference at the symptomatic stage;

Fig. 3 C), showing no significant impact of S100a9 deletion on pathological hallmarks of the disease.

4. Discussion

While our hypothesis was that deletion of S100a9 would have a positive outcome on mutant SOD1 mediated ALS disease in mice, here, we show that, if at all, it rather had a negative effect, by marginally accelerating onset and the late disease phase. In addition, since S100-A9 was reported to be mainly expressed by innate immune cells, we expected that microglial cell reactivity, in the context of the disease, would be overall reduced in hSOD1^{G93A}:S100a9-/- mice, what we, however, did not find. Several inflammatory properties mediated by S100-A9 made it a good target to be modulated in ALS, including its ability to induce chemotaxis of leukocytes and adherence of neutrophils, to activate inflammatory cells through TLR4 binding and MyD88/NFκB pathway activation, leading to proinflammatory cytokine release and production of reactive oxygen species (Ryckman et al., 2003; Vogl et al., 2007). However, in our study, deletion of S100a9 did not impact overall microglial activation or motor neuron survival in mutant SOD1 ALS mice. In AD, a recent study showed that S100-A8 aggregated prior to amyloid plaque formation in APP transgenic mice (Lodeiro et al., 2017). Moreover, the S100-A8/A9 complex is highly expressed in microglial cells surrounding amyloid plaques in AD postmortem brain tissues and S100-A9 is overexpressed in cerebrospinal fluid of AD patients (Ha et al., 2010; Kim et al., 2014; Kummer et al., 2012). In addition, the S100-A8/A9 complex drives inflammation after ischemia, emphasizing its role in several inflammatory conditions (Ziegler et al., 2009). Our results suggest that, at least in mouse models, deletion of S100a9 has rather opposite effects in ALS than in AD and ischemia models. In conclusion, although S100-A9 can play an important role in inflammation, is mainly expressed by phagocytic cells and is a microglial candidate to target in certain models with neuroinflammation, we showed that deletion of S100a9 in mutant SOD1 ALS mice did not alleviate but rather slightly exacerbated the disease. Therefore, this

suggests that the S100-A8/A9 pathway does not contribute to mutant SOD1 mediated ALS toxicity and, at least based on this mouse model, its blockage does not represent a promising strategy to slow ALS.

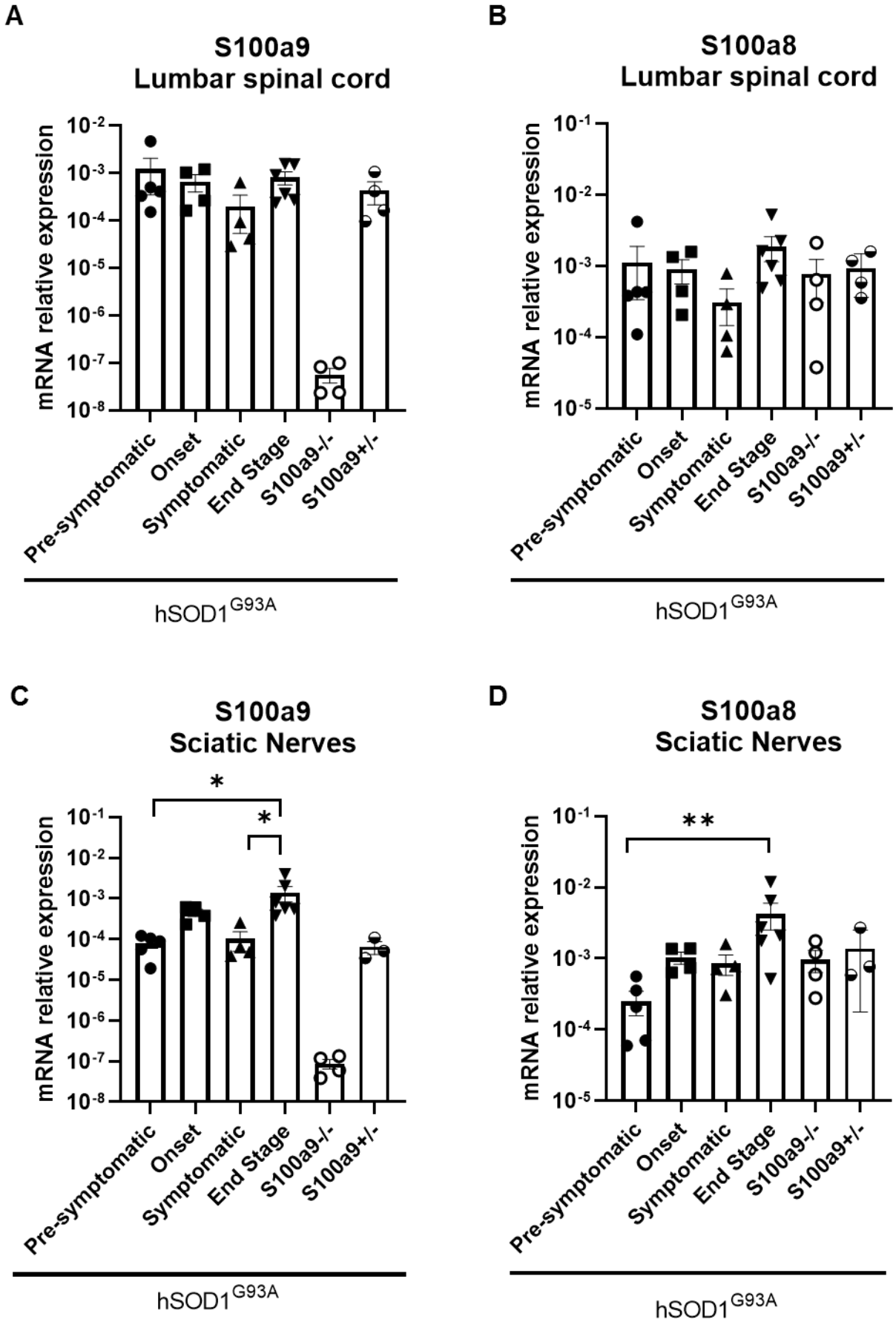

Ribon et al., Fig. 1

Fig. 1: *S100a8* and *S100a9* mRNA expression levels are not modified in lumbar spinal cords throughout the disease, but increased at end stage in sciatic nerves of hSOD1^{G93A} ALS mice.

mRNA levels of *S100a8* and *S100a9* were measured in whole lumbar spinal cords and sciatic nerves at four different disease stages in hSOD1^{G93A} ALS mice. In hSOD1^{G93A}:S100a9+/+ mice, 'Presymptomatic': 50 days of age, 'Onset': defined as the weight peak, in mean at the age of 107 days, 'Symptomatic stage': defined by 10% of weight loss, in mean at the age of 150 days, End stage: defined as complete hindlimb paralysis reached in mean at the age of 166 days, and in hSOD1^{G93A}:S100a9-/- and hSOD1^{G93A}:S100a9+/- at onset. Whole lumbar spinal cord (A, B) or sciatic nerve (C, D) tissue mRNA levels for *S100a9* (A, C) and *S100a8* (B, D) were measured by reverse-transcription quantitative PCR and normalized to the housekeeping gamma-actin *(Actg1)* gene. Results are shown relative to *Actg1* expression. Bars represent Means ± SEM for n=4 mice at every stage (except at pre-symptomatic n=5, end stage n=6 and hSOD1^{G93A}:S100a9+/- n=3 mice). * $p<0.05$, **$p<0.01$ (Kruskal-Wallis test followed by Dunnett's post-hoc test).

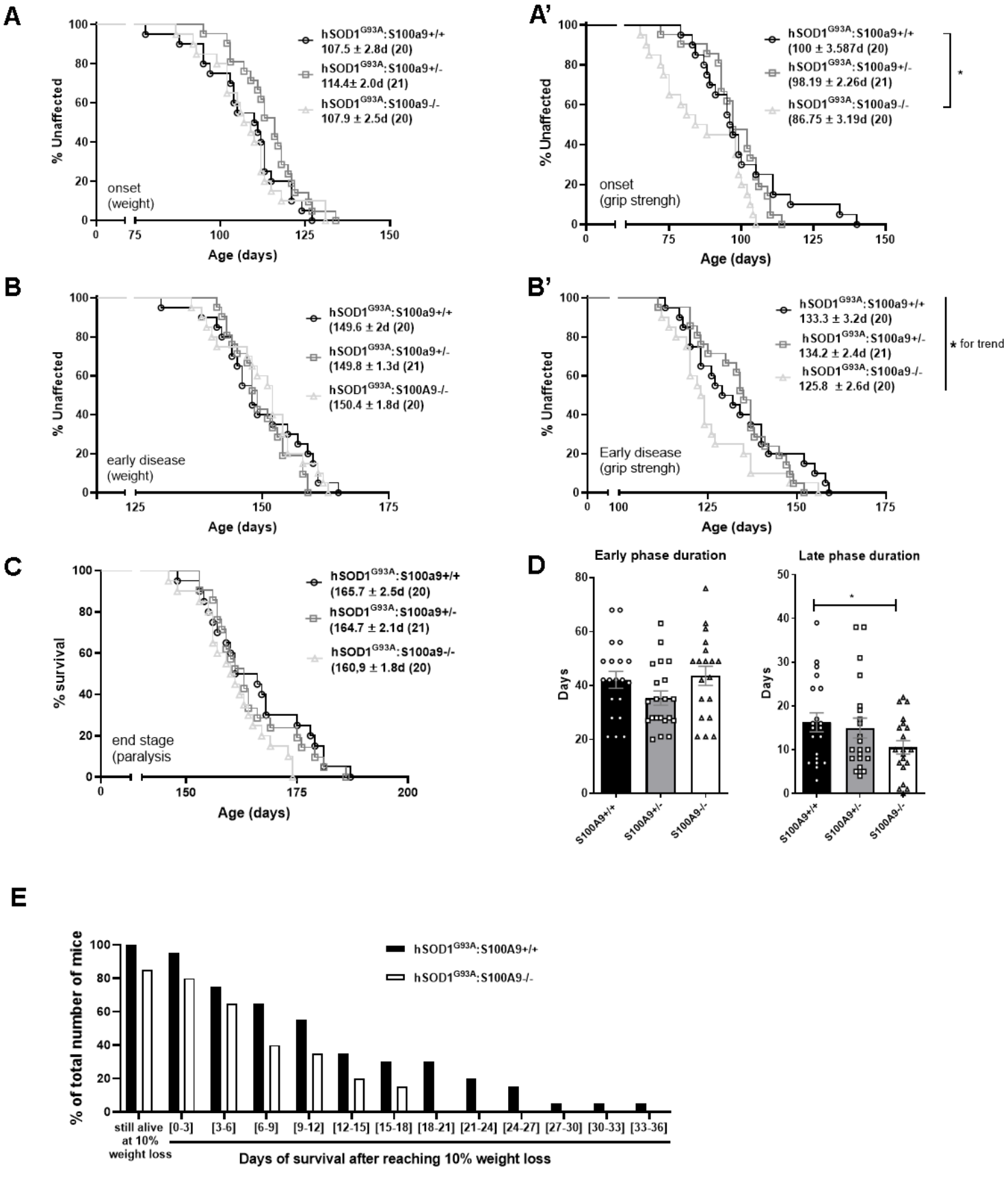
A
% Unaffected
onset
(weight)
hSOD1G93A:S100a9+/+
107.5 ± 2.8d (20)
hSOD1G93A:S100a9+/-
114.4± 2.0d (21)
hSOD1G93A:S100a9-/-
107.9 ± 2.5d (20)
Age (days)
A'
onset
(grip strengh)
hSOD1G93A:S100a9+/+
(100 ± 3.587d (20)
hSOD1G93A:S100a9+/-
(98.19 ± 2.26d (21)
hSOD1G93A:S100a9-/-
(86.75 ± 3.19d (20)
*
B
early disease
(weight)
hSOD1G93A:S100a9+/+
(149.6 ± 2d (20)
hSOD1G93A:S100a9+/-
(149.8 ± 1.3d (21)
hSOD1G93A:S100A9-/-
(150.4 ± 1.8d (20)
B'
Early disease
(grip strengh)
hSOD1G93A:S100a9+/+
133.3 ± 3.2d (20)
hSOD1G93A:S100a9+/-
134.2 ± 2.4d (21)
hSOD1G93A:S100a9-/-
125.8 ± 2.6d (20)
* for trend
C
% survival
end stage
(paralysis
hSOD1G93A:S100a9+/+
(165.7 ± 2.5d (20)
hSOD1G93A:S100a9+/-
(164.7 ± 2.1d (21)
hSOD1G93A:S100a9-/-
(160,9 ± 1.8d (20)
D
Early phase duration
Late phase duration
Days
S100A9+/+
S100A9+/-
S100A9-/-
E
% of total number of mice
hSOD1G93A:S100A9+/+
hSOD1G93A:S100A9-/-
still alive at 10% weight loss
[0-3]
[3-6]
[6-9]
[9-12]
[12-15]
[15-18]
[18-21]
[21-24]
[24-27]
[27-30]
[30-33]
[33-36]
Days of survival after reaching 10% weight loss

Fig. 2: Deletion of *S100a9* in ALS mice does not modify survival but slightly accelerates symptoms.

(A-C) Kaplan-Meier analyses of ages when onset (weight peak (A), or grip strength peak (A')), symptomatic stage (10% of weight loss (B), or 35% of grip strength loss (B')) and end stage (complete hindlimb paralysis) (C) where reached, in hSOD1^{G93A} (black), hSOD1^{G93A}:S100a9+/- (grey) and hSOD1^{G93A}:S100a9-/- (light grey) mice. Means ± SEM are indicated with number of animals (gender balance) in brackets. * $p<0.05$ (log-rank test). (D left), early disease duration corresponding to the mean of the difference between age at onset and age when reaching 10% of weight loss for each individual mouse. (D right), late disease duration, corresponding to the mean of the difference between ages at 10% of weight loss and end stage for each individual mouse. hSOD1^{G93A}:S100a9+/+ (black bars) n=20 mice, hSOD1^{G93A}:S100a9+/- (grey bar) n=21 mice and hSOD1^{G93A}:S100a9-/- (white bars) n=20 mice. Bars represent Means ± SEM. * $p<0.05$ (Student's t-test). (E) Survival duration in days after reaching 10% weight loss. Bars represent the proportion of mice still alive within the indicated time frame. hSOD1^{G93A}:S100a9+/+ (black bars) n=20 mice, and hSOD1^{G93A}:S100a9-/- (white bars) n=20 mice.

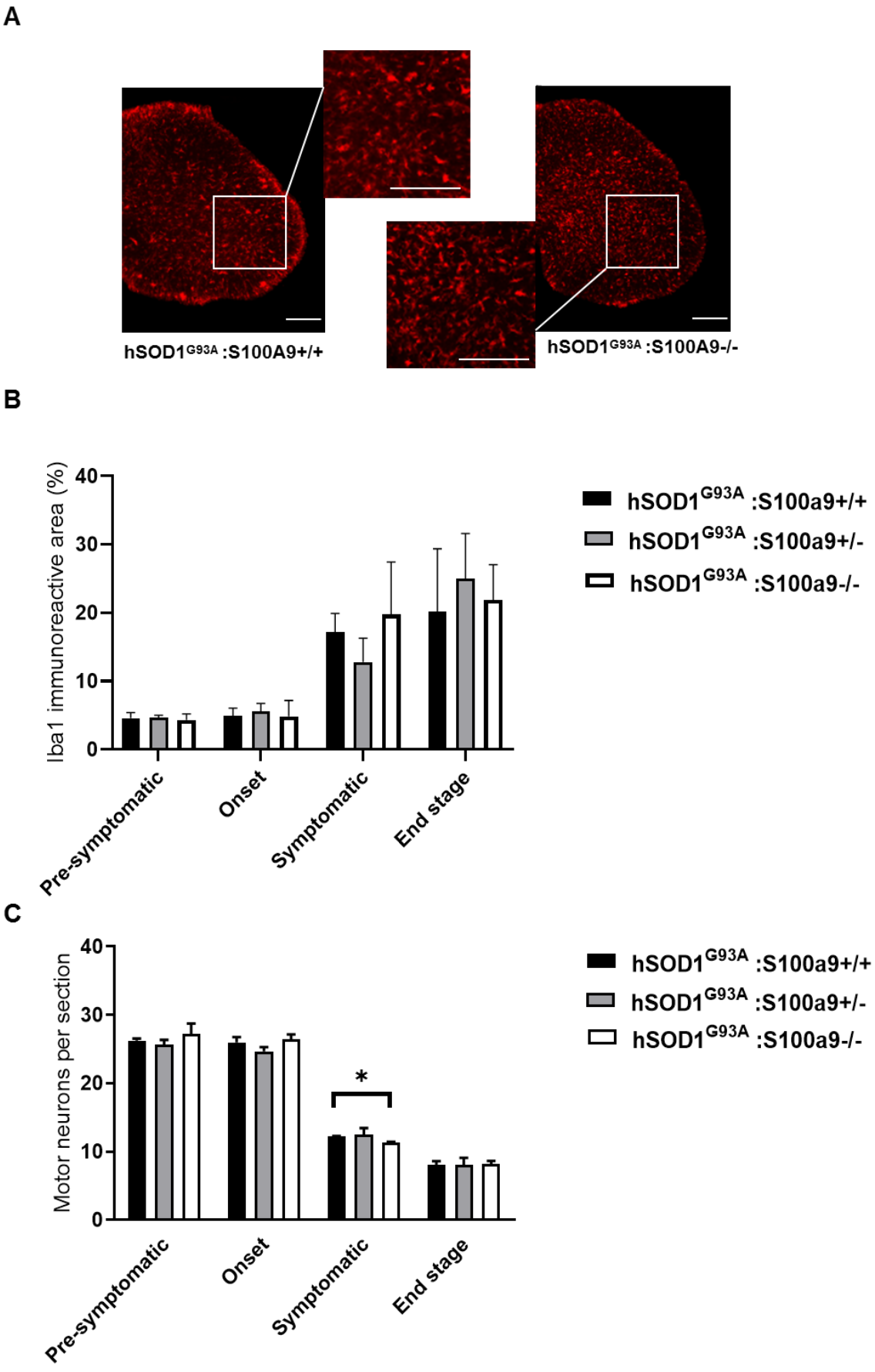

Ribon et al., Fig. 3

Fig. 3: Microglial activation and motor neuron survival are not affected by *S100a*9 deletion in hSOD^{G93A} mice.

(A) Representative pictures of lumbar spinal cord cross sections stained against Iba1 reflecting microglial activation at onset. Right panel hSOD1^{G93A}:S100A9+/+ mouse, left panel: hSOD1^{G93A}:S100A9-/- mouse. Scale bars, 100µm. (B) Microglial cell activation in lumbar spinal cord cross sections measured by anti-Iba1 fluorescent immunoreactive area. (C) Motor neuron numbers per lumbar spinal cord section. Bars represent Mean +/- SEM for n=4 mice per stage and per genotype (except for n=3 for hSOD1^{G93A}:S100a9+/- at onset for motor neuron counts), gender balance. * $p<0.05$ (mixed-effects analysis (ANOVA) followed by Tukey's post-hoc test).

Disclosure statement:

The authors declare no conflict of interest.

Data contained in the manuscript

The authors declare that the data contained in the manuscript being submitted have not been previously published, have not been submitted elsewhere and will not be submitted elsewhere while under consideration at Neurobiology of Aging.

Animals

All animal procedures (including end stage definition) were performed in accordance with the guidelines for care and use of experimental animals of the European Union and approved by the ethics committee for animal experimentation n °5 in Ile- de-France to the UMS28, Centre d'expérimentation fonctionnelle, Paris, France.

Authors approval

All author's have reviewed the content of the manuscript being submitted, approved its contents and validated the accuracy of the data.

Authors' contributions

Matthieu Ribon: Investigation, Validation, Formal Analysis, Visualization, Writing Original draft; Céline Leone: Investigation, Visualization, Validation, Formal Analysis; Aude Chiot: Investigation, Validation, Writing-Review & Editing; Félix Berriat: Investigation, Writing-Review & Editing; Martine Rampanana: Investigation, Visualization; Julie Cottin: Investigation, Visualization; Delphine Bohl: Writing-Review & Editing; Stéphanie Millecamps: Writing-Review & Editing; Christian S. Lobsiger: Conceptualization, Writing-Review & Editing; Michael T. Heneka: Conceptualization, Resources, Funding Acquisition, Writing-Review & Editing; Séverine Boillée: Supervision, Conceptualization, Funding Acquisition, Writing-Review & Editing.

Acknowledgements

We kindly thank Pr. Thomas Vogl (Institute of Immunolgy Münster, Germany), Drs. Olivier Dussurget and Marie-Anne Nahori (Pasteur Institute, Paris, France) for providing S100a9-/- mice. We thank the technical staff from our animal housing facility (UMS28, Centre d'expérimentation fonctionnelle, Paris, France) and the following ICM core facilities (Paris, France): iGenSeq, His-tomics, ICM.Quant (which received ANR-10-IAIHU-06 funding). This study was funded by: ERA-NET NEURON (ANR-14-NEUR-0 0 03-02), ARSLA, Fondation Thierry Latran, NRJ-Institut de France, l'ARMC, S.L.A.F.R., 'La longue route des malades de la SLA', 'Un pied devant l'autre' and private donors to ALS at the ICM.

References

Akiyama, H., Ikeda, K., Katoh, M., McGeer, E.G., McGeer, P.L., 1994. Expression of MRP14, 27E10, interferon-alpha and leukocyte common antigen by reactive microglia in postmortem human brain tissue. J. Neuroimmunol. 50, 195–201.

Beers, D.R., Henkel, J.S., Xiao, Q., Zhao, W., Wang, J., Yen, A.A., Siklos, L., McKercher, S.R., Appel, S.H., 2006. Wild-type microglia extend survival in PU.1 knockout mice with familial amyotrophic lateral sclerosis. Proc. Natl. Acad. Sci. U.S.A. 103, 16021–16026.

Boillée, S., Yamanaka, K., Lobsiger, C.S., Copeland, N.G., Jenkins, N.A., Kassiotis, G., Kollias, G., Cleveland, D.W., 2006. Onset and progression in inherited ALS determined by motor neurons and microglia. Science 312, 1389–1392.

Chiot, A., Zaïdi, S., Iltis, C., Ribon, M., Berriat, F., Schiaffino, L., Jolly, A., de la Grange, P., Mallat, M., Bohl, D., Millecamps, S., Seilhean, D., Lobsiger, C.S., Boillée, S., 2020. Modifying macrophages at the periphery has the capacity to change microglial reactivity and to extend ALS survival. Nat Neurosci 23, 1339–1351.

Donato, R., Cannon, B.R., Sorci, G., Riuzzi, F., Hsu, K., Weber, D.J., Geczy, C.L., 2013. Functions of S100 proteins. Curr. Mol. Med. 13, 24–57.

Ehrchen, J.M., Sunderkötter, C., Foell, D., Vogl, T., Roth, J., 2009. The endogenous Toll–like receptor 4 agonist S100A8/S100A9 (calprotectin) as innate amplifier of infection, autoimmunity, and cancer. Journal of Leukocyte Biology 86, 557–566.

Gurney, M.E., Pu, H., Chiu, A.Y., Dal Canto, M.C., Polchow, C.Y., Alexander, D.D., Caliendo, J., Hentati, A., Kwon, Y.W., Deng, H.X., 1994. Motor neuron degeneration in mice that express a human Cu,Zn superoxide dismutase mutation. Science 264, 1772–1775.

Ha, T.-Y., Chang, K.-A., Kim, J. a, Kim, H.-S., Kim, S., Chong, Y.H., Suh, Y.-H., 2010. S100a9 knockdown decreases the memory impairment and the neuropathology in Tg2576 mice, AD animal model. PLoS ONE 5, e8840.

Kim, H.J., Chang, K.-A., Ha, T.-Y., Kim, J., Ha, S., Shin, K.-Y., Moon, C., Nacken, W., Kim, H.-S., Suh, Y.-H., 2014. S100A9 knockout decreases the memory impairment and neuropathology in crossbreed mice of Tg2576 and S100A9 knockout mice model. PLoS ONE 9, e88924.

Kummer, M.P., Vogl, T., Axt, D., Griep, A., Vieira-Saecker, A., Jessen, F., Gelpi, E., Roth, J., Heneka, M.T., 2012. Mrp14 deficiency ameliorates amyloid β burden by increasing microglial phagocytosis and modulation of amyloid precursor protein processing. J. Neurosci. 32, 17824–17829.

Lodeiro, M., Puerta, E., Ismail, M.-A.-M., Rodriguez-Rodriguez, P., Rönnbäck, A., Codita, A., Parrado-Fernandez, C., Maioli, S., Gil-Bea, F., Merino-Serrais, P., Cedazo-Minguez, A., 2017. Aggregation of the Inflammatory S100A8 Precedes Aβ Plaque Formation in Transgenic APP Mice: Positive Feedback for S100A8 and Aβ Productions. J Gerontol A Biol Sci Med Sci 72, 319–328.

Manitz, M.-P., Horst, B., Seeliger, S., Strey, A., Skryabin, B.V., Gunzer, M., Frings, W., Schönlau, F., Roth, J., Sorg, C., Nacken, W., 2003. Loss of S100A9 (MRP14) results in reduced interleukin-8-induced CD11b surface expression, a polarized microfilament system, and diminished responsiveness to chemoattractants in vitro. Mol. Cell. Biol. 23, 1034–1043.

Mesci, P., Zaïdi, S., Lobsiger, C.S., Millecamps, S., Escartin, C., Seilhean, D., Sato, H., Mallat, M., Boillée, S., 2015. System xC− is a mediator of microglial function and its deletion slows symptoms in amyotrophic lateral sclerosis mice. Brain 138, 53–68.

Passey, R.J., Williams, E., Lichanska, A.M., Wells, C., Hu, S., Geczy, C.L., Little, M.H., Hume, D.A., 1999. A Null Mutation in the Inflammation-Associated S100 Protein S100A8 Causes Early Resorption of the Mouse Embryo. J. Immunol. 163, 2209–2216.

Ryckman, C., Vandal, K., Rouleau, P., Talbot, M., Tessier, P.A., 2003. Proinflammatory activities of S100: proteins S100A8, S100A9, and S100A8/A9 induce neutrophil chemotaxis and adhesion. J. Immunol. 170, 3233–3242.

Silverman, J.M., Fernando, S.M., Grad, L.I., Hill, A.F., Turner, B.J., Yerbury, J.J., Cashman, N.R., 2016. Disease Mechanisms in ALS: Misfolded SOD1 Transferred Through Exosome-Dependent and Exosome-Independent Pathways. Cell Mol Neurobiol 36, 377–381.

Urushitani, M., Sik, A., Sakurai, T., Nukina, N., Takahashi, R., Julien, J.-P., 2006. Chromogranin-mediated secretion of mutant superoxide dismutase proteins linked to amyotrophic lateral sclerosis. Nat Neurosci 9, 108–118.

Vogl, T., Tenbrock, K., Ludwig, S., Leukert, N., Ehrhardt, C., van Zoelen, M.A.D., Nacken, W., Foell, D., van der Poll, T., Sorg, C., Roth, J., 2007. Mrp8 and Mrp14 are

endogenous activators of Toll-like receptor 4, promoting lethal, endotoxin-induced shock. Nat. Med. 13, 1042–1049.

Wang, Siwen, Song, R., Wang, Z., Jing, Z., Wang, Shaoxiong, Ma, J., 2018. S100A8/A9 in Inflammation. Front. Immunol. 9, 1298.

Zhang, Y., Chen, K., Sloan, S.A., Bennett, M.L., Scholze, A.R., O'Keeffe, S., Phatnani, H.P., Guarnieri, P., Caneda, C., Ruderisch, N., Deng, S., Liddelow, S.A., Zhang, C., Daneman, R., Maniatis, T., Barres, B.A., Wu, J.Q., 2014. An RNA-Sequencing Transcriptome and Splicing Database of Glia, Neurons, and Vascular Cells of the Cerebral Cortex. J. Neurosci. 34, 11929–11947.

Ziegler, G., Prinz, V., Albrecht, M.W., Harhausen, D., Khojasteh, U., Nacken, W., Endres, M., Dirnagl, U., Nietfeld, W., Trendelenburg, G., 2009. Mrp-8 and -14 mediate CNS injury in focal cerebral ischemia. Biochimica et Biophysica Acta (BBA) - Molecular Basis of Disease, Mitochondrial Disease 1792, 1198–1204.

Supplementary Information

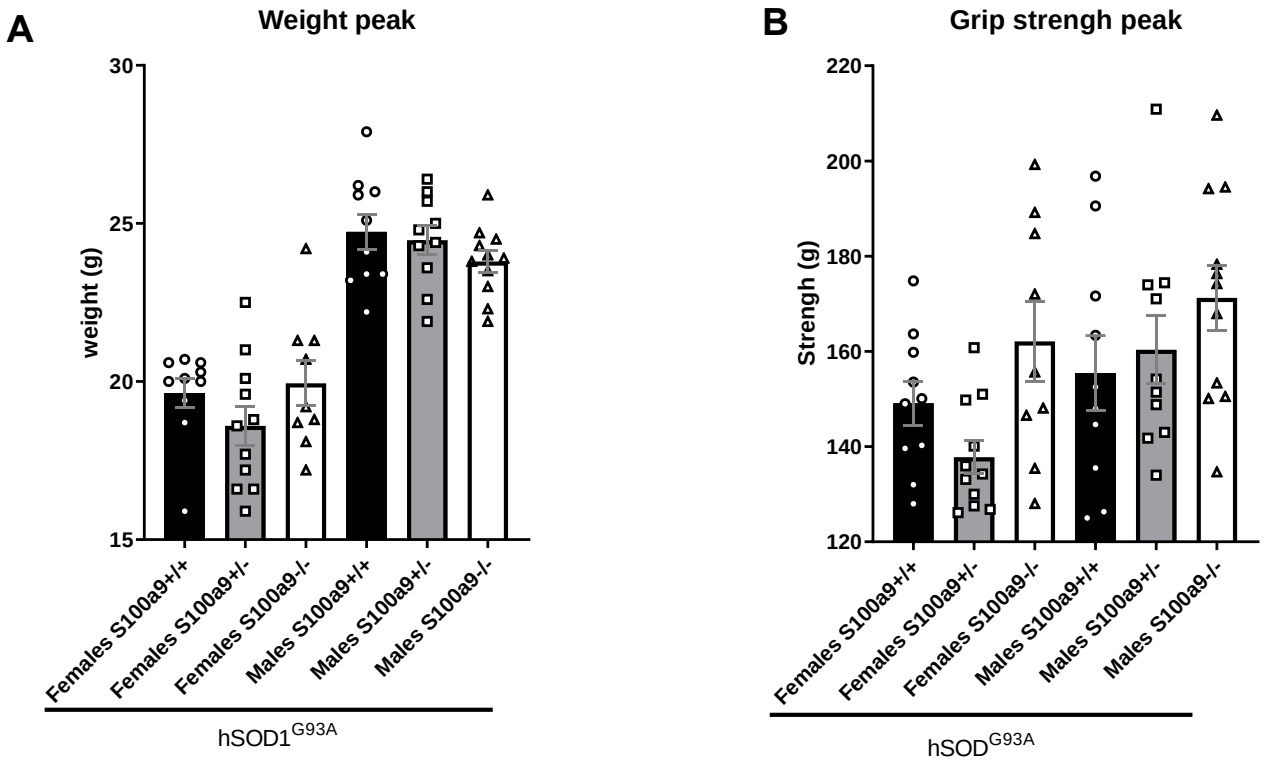

Supplementary Fig.1: Maximum weight and grip strength for each mouse.

Mice were followed weekly from the pre-symptomatic stage until disease end stage. Histograms represent maximum weight (A) and grip strength score (B) used to determine disease onset. hSOD1^{G93A}:S100a9+/+ (black bar), hSOD1^{G93A}:S100a9+/- (grey bar) and hSOD1^{G93A}:S100a9-/- (white bar). Bars represent Means ± SEM for n=9 to 11 mice

Material and methods.

Animals: All mice (equally gender mixed) were on a C57Bl6/J genetic background (Janvier, Le-Genest-St-Isle, France). SOD1 transgenic mice were hSOD1^{G93A} mice (B6.Cg-Tg(SOD1*G93A)1Gur/J - 004435, Jackson Laboratory). These mice were hemizygous for a 12kb genomic fragment encoding the human mutated SOD1 gene under its endogenous promoter and develop an ALS-like phenotype including a progressive paralysis (Gurney et al., 1994). hSOD1^{G93A}:S100a9+/+ (n=20), hSOD1^{G93A}:S100a9+/- (n=21) or hSOD1^{G93A}:S100a9-/- (n=20) (F2 generation) were obtained by crossing hSOD1^{G93A} males with S100A9-/- females

(Manitz et al., 2003) (provided by Dr. Thomas Vogl, Institute of Immunolgy Münster, Germany and Drs. Olivier Dussurget and Marie-Anne Nahori, Pasteur Institute, Paris, France) and then hSOD1^{G93A} :S100a9+/- males with S100a9+/- females. Mice carrying the human SOD1 transgene were identified by PCR screening of tail DNA allowing the simultaneous amplification of human and mouse Sod1 fragments using mouse SOD1 forward primer (5'-GTTACATATAGGGGTTTACTTCATAATCTG-3'), human SOD1 forward primer (5'-CCAAGATGCTTAACTCTTGTAATCAATGGC-3') and mouse and human SOD1 reverse primer (5'-CAGCAGTCACATTGCCCAGGTCTCCAACATG-3'), resulting in ~800bp mouse and ~600bp human SOD1 PCR products. S100a9 mouse genotypes were determined by PCR screening of tail DNA using mouse S100a9 wild type (WT) forward primer 5'-CCATATCCCAGTGTTGGTGAC-3', Neomycin forward primer 5'-CGCCTTCTATCGCCTTCTTGA-3' and S100a9 mouse reverse primer 5'-GTCTTTAACCAGGGACTAGG-3', resulting in ~620bp WT S100a9 and ~660bp invalidated S100a9 PCR products.

All animal procedures (including end stage definition) were performed in accordance with the guidelines for care and use of experimental animals of the European Union and approved by the ethics committee for animal experimentation n°5 in Ile-de-France to the UMS28, Centre d'expérimentation fonctionnelle, Paris, France.

Disease stage analysis. Mice were followed weekly from the pre-symptomatic stage (50 days) until disease end stage (around 165 days). Mice were followed for signs of paralysis, grip strength (Bioseb, grip test; average of three consecutive weekly measures) and weigh determined weekly as an objective and unbiased measure of the disease course. Grip strength measures were performed until the animal was too weak to perform it. Disease time points were defined as in (Chiot et al., 2020; Mesci et al., 2015) as follows: time of disease onset was retrospectively determined as the time when mice reached either peak body weight or peak grip strength; the symptomatic time point was defined as the age at which the animals

had lost 10% of their maximal weight or 35% of their maximal grip strength, which is accompanied by gait alterations and failure of hindlimb splaying reflex without obvious signs of paralysis; the symptomatic stage was followed by the appearance of progressive paralysis until end stage, which was defined by paralysis so severe that the animal could not right itself within 20 seconds when placed on its side, an endpoint frequently used for SOD1 mutant expressing mice. Mean ages ± SEM of the different disease stages in our $SOD1^{G93A}$ colony (S100a9+/+) defined by weight measurement were as follows: disease onset: 107.5 ± 2.8 days, symptomatic stage: 149.6 ± 2 days and disease end stage: 165.7 ± 2.5 days.

Mouse tissue collection. For immunostaining: Mice were euthanized with Penthobarbital and transcardially perfused with 0.1M Phosphate Buffered Saline (PBS) followed by ice-cold 4% paraformaldehyde (PFA) in PBS. Sciatic nerves, and lumbar spinal cords were collected and post-fixed in 4% PFA for 4 hours. Tissues were then cryoprotected in 30% sucrose in PBS for 48 hours before freezing in isopentane at -40C.

For qPCR: Mice were euthanized with Penthobarbital. Lumbar spinal cords were flushed using 0.1M PBS, and the two whole left and right sciatic nerves (from the gastrocnemius muscles to the spine vertebrae) were collected and pooled and then immediately frozen in liquid nitrogen.

RNA extraction and real-time PCR. Since S100a8 and S100a9 are mainly expressed by microglia in the CNS, are not expressed by motor neurons (in control or ALS mice), and astrocytes do not regulate S100a8 or S100a9 mRNA in $hSOD1^{G93A}$ mice (Lobsiger et al., 2007; Miller et al., 2018; Zhang et al., 2014), S100a8 or S100a9 mRNA regulations measured by RT-qPCR performed in whole lumbar spinal cord tissues should represent microglial expression. RNA was extracted from whole lumbar mouse spinal cords and sciatic nerves (n=4 at every stage, except pre-symptomatic, n=5, end stage with n=6, and $hSOD1^{G93A}$:S100a9+/-, n=3 mice), using an OMNI international tissue master 125 tissue homogenizer in Qiazol reagent (Qiagen), using the Qiagen RNeasy mini lipid kit followed by

a DNAse treatment (Qiagen). RNA concentrations were determined by Nanodrop. Reverse transcription was performed with Superscript IV (Life Technologies) using 1µg of total RNA using random hexamers. qPCRs were performed with LightCycler® 480 SYBR Green I Master (Roche), 200 nM of primers on Roche LightCycler® 480 and LightCycler® 96 instruments. cDNA final dilution was 1/20. The relative expression levels of each mRNA were calculated using the ddCt method normalized to gamma-actin (*Actg1*). We verified that mRNA for the normalizer *Actg1* were stably expressed over the disease course with a small difference in presymptomatic SOD1^{G93A} tissues compared to symptomatic tissues that could not account for the differences measured for S100a8 and S100a9. The presence of a unique product of the correct size was verified by melting curve analysis.

qPCR Primers. S100a9 primers: forward 5'-CTCTAGGAAGGAAGGACACC-3', reverse 5'-GCCATCAGCATCATACACTC-3'. S100a8 primers: forward 5'-CCTTTGTCAGCTCCGTCTTC-3', reverse primer: 5'-CATCAATGAGGTTGCTCAAGG-3'. Actg1 (gamma-actin): forward: 5'-TGGATCAGCAAGCAGGAGTATG-3', reverse: 5'-CCTGCTCAGTCCATCTAGAAGCA-3'

Motor neuron counts. Motor neuron numbers were determined from 30µm serial sections across the entire lumbar spinal cord and counted in the spinal cord ventral horn. Counts were performed on every 12th cresyl violet acetate-stained section corresponding to a total of 16–22 sections per animal for n=4 mice per genotype and time point or n=3 for hSOD1^{G93A}:S100a9+/- at onset.

Microglial cell activation. Lumbar spinal cord sections: 30µm transverse cryosections were incubated overnight at room temperature with rabbit anti-Iba1 antibodies (1:500, Wako Chemicals) in PBS with 0.3% Triton X100. The staining was revealed using species-specific Alexa Fluor-594 secondary antibodies (1:1000, Life Technologies). Pictures of lumbar spinal cords were obtained using an Axioscan scanner (Zeiss). All the analyses were performed with Image-J software (Fiji). A common microglial cell detection threshold was set up for every

section and the % area (measuring the Iba1+ fluorescent immunoreactivity area in the parenchyma) was calculated. Measures were realized in every 24th lumbar spinal cord section corresponding to a total of 7-12 sections per animal for n=4 mice per genotype and time point.

Statistical analysis. All data are presented as Mean +/- SEM (except Fig. 2 E, relative number (%)), the statistics were performed using GraphPad software Prism 8. Kruskal-Wallis followed by Dunnett's post-hoc analysis of mean differences was used to compare multiple groups after Normality test (Fig. 1, Supplementary Fig. 1); Mixed effect analysis (two-way ANOVA with missing values) followed by Tukey's post-hoc analysis was used to compare each mean to a control mean after Normality test (Fig. 3); Student's t-tests, two-tailed and unpaired, were used to compare means of two groups after Normality test (Fig. 2 D) and Log-rank tests were performed to analyze survival curves (Fig. 2 A-C).

Supplementary References

Chiot, A., Zaïdi, S., Iltis, C., Ribon, M., Berriat, F., Schiaffino, L., Jolly, A., de la Grange, P., Mallat, M., Bohl, D., Millecamps, S., Seilhean, D., Lobsiger, C.S., Boillée, S., 2020. Modifying macrophages at the periphery has the capacity to change microglial reactivity and to extend ALS survival. Nat Neurosci 23, 1339–1351.

Lobsiger, C.S., Boillée, S., Cleveland, D.W., 2007. Toxicity from different SOD1 mutants dysregulates the complement system and the neuronal regenerative response in ALS motor neurons. Proc Natl Acad Sci U S A 104, 7319–7326.

Mesci, P., Zaïdi, S., Lobsiger, C.S., Millecamps, S., Escartin, C., Seilhean, D., Sato, H., Mallat, M., Boillée, S., 2015. System xC− is a mediator of microglial function and its deletion slows symptoms in amyotrophic lateral sclerosis mice. Brain 138, 53–68.

Miller, S.J., Glatzer, J.C., Hsieh, Y.-C., Rothstein, J.D., 2018. Cortical astroglia undergo transcriptomic dysregulation in the G93A SOD1 ALS mouse model. J Neurogenet 32, 322–335.